43rd AIAA/ASME/SAE/ASEE Joint Propulsion Conference & Exhibit
8 - 11 July 2007, Cincinnati, OH

AIAA 2007-5306

Number Density Distributions of Xenon Atom in Hall Thruster Plumes

Makoto Matsui*, Shigeru Yokota†, Daichi Sako‡, Kimiya Komurasaki§, Yoshihiro Arakawa**
The University of Tokyo, Tokyo, 113-8656, JAPAN

Laser absorption spectroscopy was applied to a magnetic layer type hall thruster plume in the different ambient pressure conditions. An influence of the ambient pressure on the number density measurement was evaluated. As a result, the measured number density was found to contain the background xenon. Then, the number density distribution of the propellant xenon was estimated separately from the background one.

Nomenclature

A	=	Einstein coefficient, s^{-1}
g	=	statistical weight
h	=	Planck's constant, J.s
I	=	probe laser intensity, mW/mm^2
I_0	=	incident laser intensity, mW/mm^2
k	=	absorption coefficient, m^{-1}
k_B	=	Boltzmann constant, J/K
K	=	integrated absorption coefficient, GHz m^{-1}
n	=	number density, m^{-3}
r	=	radial coordinate, mm
R	=	plume radius, mm
T	=	translational temperature, K
T_e	=	electron temperature, eV
x	=	coordinate in the laser pass direction, mm
y	=	probe beam position, mm
z	=	axial coordinate, mm
ΔE	=	energy gap, eV
λ	=	wavelength, nm
ν	=	laser frequency, Hz
ν_0	=	center absorption frequency, Hz

Subscript

i	=	absorption state
j	=	excited state
tot	=	total states

I. Introduction

Hall thrusters are one of the promising thrusters of satellites for orbit transfer or North/South station keeping missions because it produces high thrust efficiency, exceeding 50%, with a specific impulse range of 1000-3000 s and a higher ion beam density than ion thrusters because of the existence of electrons in the ion acceleration

* JSPS Research Fellow, Department of Aeronautics and Astronautics, matsui@al.t.u-tokyo.ac.jp. Member AIAA.
† Graduate student, Department of Aeronautics and Astronautics, Student Member AIAA.
‡ Graduate student, Department of Aeronautics and Astronautics.
§ Associate Professor, Department of Advanced Energy, Member AIAA.
** Professor, Department of Aeronautics and Astronautics, Member AIAA.

zone. This is because a moderate magnetic field is applied in the acceleration zone, causing the magnetization of the electrons and not the ions.[1-3]. Hence, several types of Hall thrusters are actively developed in Russia, USA, EU and Japan[4-10].

In their practical use in a spacecraft, the interactions between the plume of the thruster and the host spacecraft cause serious problems[11-13]. High-energy main beam ions generated and accelerated in the acceleration channel collide with unionized propellant atoms in the plume, resulting in the production of low-energy ions and high-energy atoms by charge exchange reaction (CEX). These CEX ions propagate in the radial and upstream directions because of the potential distribution near the spacecraft. The backflow of CEX ions becomes a contamination source causing erosion, sputtering, degradation, increment of temperature and potential change of solar arrays or spacecraft surfaces.

Recently, a plume shield has been developed to protect the spacecraft from CEX ions. The plume shield developed by Mitsubishi Electric Corporation intercepts ions with higher angle beyond 45 degree[14]. Then, it is important to clarify a production mechanism of CEX reactions to evaluate the shields performances and optimization. Plume characteristics have been a hot subject and investigated experimentally in ground-based facilities[15-20] and even in an actual flight test[21] as well as numerical calculations[22-25]. Because most of measurements, however, are conducted by intrusive probe methods such as electrostatic probes, energy analyzers and mass spectrometers, measurements near the thruster exit are difficult for their disturbances, where CEX reactions would most frequently take place[14-20]. The plume properties near the thruster exit are also useful for initial conditions of numerical calculations.

In our previous research, laser absorption spectroscopy (LAS) and single probe measurements were applied to a magnetic-layer-type hall thruster plume developed at the University of Tokyo[9, 26]. However, measured number density of xenon might be overestimated due to an influence of background xenon. In this study, number density distributions of xenon atom were measured in two different ambient pressure conditions to evaluate the influence of the background xenon on the measurement. Then, the number density distribution of the propellant xenon atom was estimated separately from the background one.

II. Theory of Laser Absorption Spectroscopy

Laser absorption spectroscopy has some superiority to other non-intrusive spectroscopes such as emission and LIF: 1) it is applicable to optically thick plasma, and 2) absolute calibration using a standard light source or a density reference cell is not necessary. Moreover, 3) the measurement system is portable when a diode laser is used[27].

The relationship between the laser intensity and the absorption coefficient is expressed by as[28],

$$\frac{\mathrm{d}I}{\mathrm{d}x} = -k(x, y, \nu)I \ . \tag{1}$$

The pass integrated absorption coefficient $K(y)$ is obtained by,

$$K(y) = \int k(x, y, \nu) d\nu dx \ . \tag{1}$$

Because distributions of absorption properties in plumes would be axisymmetric, local integrated absorption coefficient $K(r)$ with the radial coordinate r is obtained by the Abel inversion expressed as[29],

$$K(r) = \frac{1}{\pi}\int_r^R \frac{d(K(\mathrm{y}))}{dy}\frac{dy}{\sqrt{y^2 - r^2}} \ . \tag{2}$$

Assuming Boltzmann relation between absorbing and excited states, integrated absorption coefficient $K(r)$ is expressed as a function of the number density at the absorbing state $n_i(r)$ as[28],

$$K(r) = \frac{\lambda^2}{8\pi}\frac{g_j}{g_i}A_{ji}n_i(r)\left[1 - \exp\left(-\frac{\Delta E_{ij}}{k_\mathrm{B}T_\mathrm{e}}\right)\right]. \tag{3}$$

Assuming Boltzmann relations among all excited states, total number density n_{tot} is deduced from measured number density as,

$$n_{\text{tot}} = \frac{n_i}{g_i} \sum_l g_l \exp\left(-\frac{\Delta E_{li}}{k_B T_e}\right). \tag{4}$$

Here summation l is taken for all states[30]. In this study, an absorption line from the meta-stable xenon atom at 823.16nm ($6s[3/2]^0{}_2 \rightarrow 6p[3/2]_2$) is targeted.

III. Experimental Setup

A. Magnetic-layer-type Hall thruster

Figures 1 and 2 show a cross section of a magnetic-layer-type Hall thruster and its photo in operation. The inner and outer diameters of the acceleration channel are 48 and 62 mm, respectively. An acceleration channel wall was made of BN. The anode is located at 21 mm, upstream end of the acceleration channel. A solenoid coil is set at the center of the thruster to apply a radial magnetic field in the acceleration channel. The magnetic flux density is varied by changing the coil current. There is no outer coil because a uniform magnetic field distribution is maintained along the azimuthal direction. A hollow cathode (7HCN-001-001; Veeco-Ion Tech Inc.) was used as an electron source and a neutralizer. A vacuum chamber of 2 m diameter by 3 m length was used in the experiments. The pumping system comprised a diffusion pump (37000 l/s), a mechanical booster pump (2800 l /s), and two rotary pumps (250 l /s). Two operation conditions are tabulated in Table 1. The ambient pressure was changed by supplying the xenon gas in the chamber.

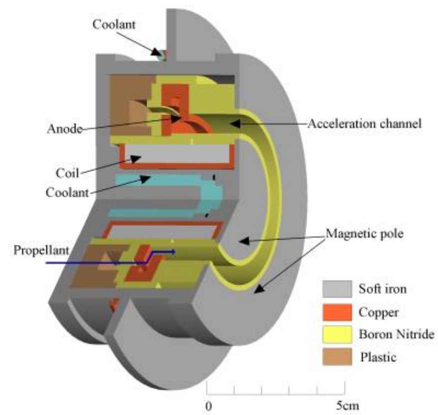

Fig. 1 Cross section of a magnetic layer type Hall thruster.

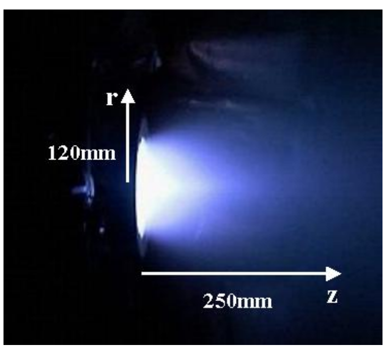

Fig. 2 A photo of a Hall thruster plume.

Table 1 Operation conditions.

Parameter	Normal p_{amb}	High p_{amb}
Propellant gas	Xe: 1.0 Aeq	Xe: 1.0 Aeq
Ambient gas	-	Xe: 0.4 Aeq
Discharge voltage	260 V	260 V
Discharge current	1.2 A	1.2 A
Applied magnetic field	11.2 mT	11.2 mT
Ambient pressure	2.77 x10^{-3} Pa	4.37x10^{-3} Pa

B. Measurement System

Figure 3 shows a schematic of the measurement system. A single longitudinal mode diode-laser (HL8325G; HITACHI Ltd., LDC205; Thorlabs Inc.) was used as the laser oscillator. The laser frequency monitored by a spectrometer (PMA50; Hamamatsu Photonics K.K.) was roughly matched to the absorption one by temperature control (TED200; Thorlabs Inc.). Then, it was scanned over the absorption line shape by current modulation with a function generator. The modulation frequency and width were 1 Hz and 30 GHz, respectively. An etalon was used as a fine wave-meter. Its free spectral range was 1 GHz.

The probe beam was guided into the vacuum chamber through a multimode optical fiber. The fiber output was mounted on a two-dimensional traverse stage to scan the plume in the radial and axial direction. The spatial resolution

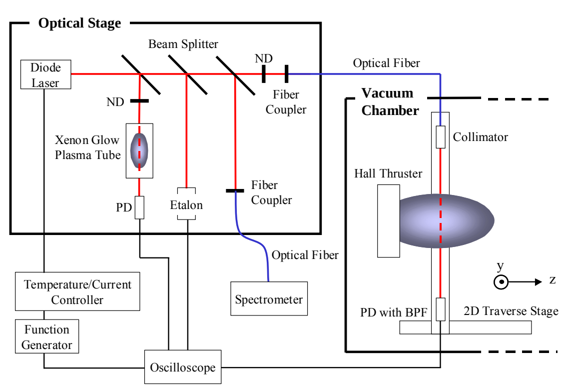

Fig. 3 Measurement system.

determined by the photo detector area was 1 mm. To reduce plasma emission, a band pass filter, whose FWHM was 10 nm, was used. As a reference, absorption signal in glow discharge plasma was also monitored. Its input power, discharge voltage and ambient pressure were 1.5 mW, 500 V, and xenon 79 Pa, respectively. All signals were recorded using a digital oscilloscope (DL708; Yokogawa Co.) with 10-bit resolution Measurement range is r<120 mm and z<200 mm as shown in Fig.3. Here, r and z are the radial and axial coordinates.

IV. Results and Discussion

A. Data Processing

Figure 4 shows transmitted laser intensity signals of the plume and glow plasma and an etalon signal. At each measurement point, eight profiles were recorded. Absorbance was obtained from normalization of the frequency and the transmitted laser intensity by the etalon signal and the laser intensity without absorption. Then pass-integrated absorption coefficients were obtained by numerical integral of the absorbance. Figure 5 shows the distributions of the pass-integrated absorption coefficients in two pressure conditions at z=20mm. As seen in this figure, the coefficients in the high pressure are larger than those in normal one. Then, the number density distributions were deduced by the Abel inversion.

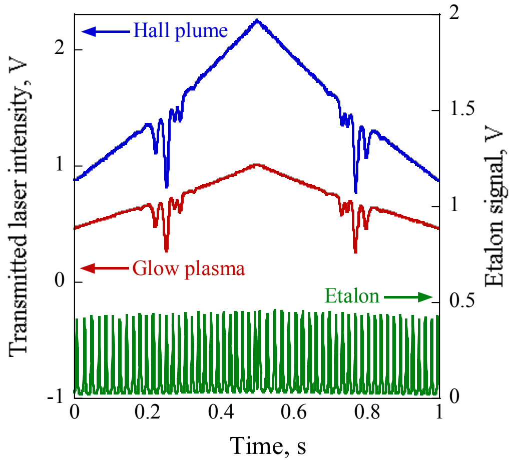

Fig. 4 Transmitted laser intensity signals of Hall plume and glow plasma and etalon signal.

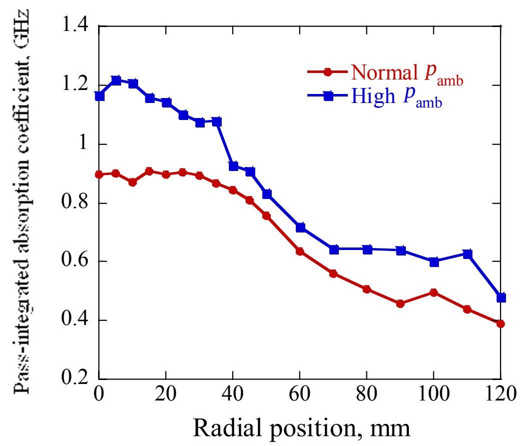

Fig. 5 Distributions of pass-integrated absorption coefficients at different ambient pressure, z=20mm.

B. Number Density Distribution

Figure 6 shows measured number density distributions of meta-stable xenon atom in the normal pressure condition. The distribution has annular peak at the acceleration channel exit and then the peak moves on the axis in the downstream. Similar distribution was obtained in the high pressure condition. Then, the distribution of the background meta-stable xenon in the normal pressure condition was deduced from the difference in the two conditions, as shown in Fig.7. The distribution has a peak on the axis and the average ratio of the background xenon to the total one was around 76%.

The total number density distribution of propellant xenon was deduced from the measured meta-stable and the electron temperature distributions using Eq. (4). Figure 8 shows deduced total number density distribution. The maximum density is $1.48 \times 10^{19} m^{-3}$ at the channel exit. Although the distribution was still directional on the axis, the decrease of the number density became rapidly. As a result, the distance whose number density was 1/e of the maximum was 50mm.

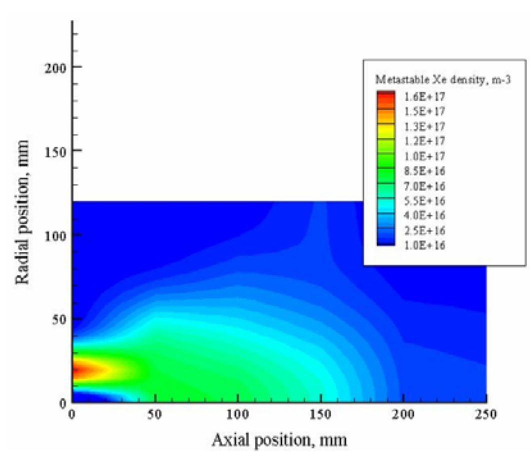

Fig. 6 Number density distribution of meta-stable xenon atom in the normal pressure condition.

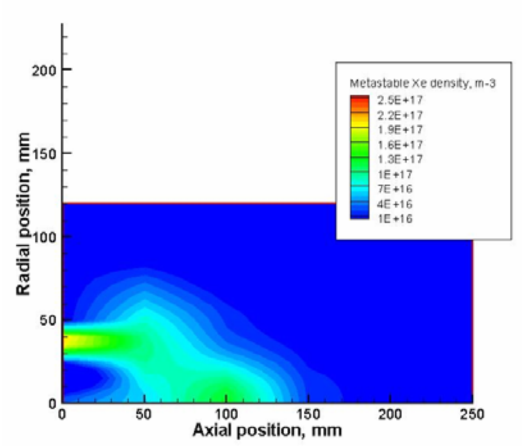

Fig. 7 Number density distribution of ambient xenon.

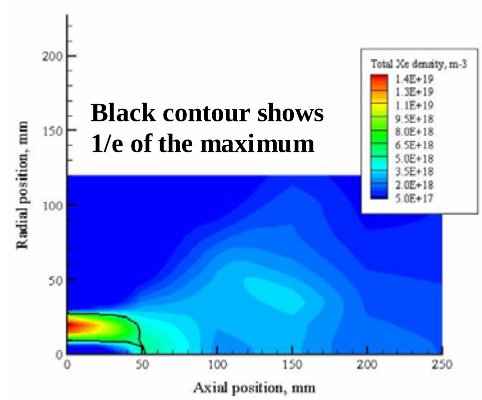

Fig. 8 Number density distribution of total propellant xenon atom.

V. Conclusion

Laser absorption spectroscopy was applied to a magnetic layer type hall thruster plume using an absorption profile of XeI 823.16 nm. The influence of the background xenon on the measurement of the propellant one was evaluated by comparing two different ambient pressure conditions. Then, the total number density of the propellant xenon was deduced from the measured meta-stable number density and the electron temperature, assuming the Boltzmann equilibrium between meta-stable and the other states. As a result, the maximum number density was 1.48×10^{19} m^{-3} at the channel and it decreased to 1/e at 50mm from the exit.

Acknowledgments

This work was partially supported by a Grand-in-Aid for Scientific Research (S), No.16106012 and for Research Fellowships of the Japan Society for the Promotion of Science for Young Scientists, 18-09885, 2006 sponsored by the Ministry of Education, Culture, Sports, Science and Technology in Japan

References

[1]Bober A., Maslennikov, N., Day, M., Popov, G. and Rylov, Yu., "Development and Application of Electric Propulsion Thruster in Russia," Proceedings of the 23rd International Electric Propulsion Conference, IEPC 93-001, 1993.

[2]Saccoccia, G., "Introduction to the European Activities in Electric Propulsion," Proceedings of the 28th International Electric Propulsion Conference, IEPC 03-341, 2003.

[3]Blandino, J., "The Year in Review, Electric Propulsion," Aerospace America, Dec. 2003, pp. 60, 61.

[4]Kim, V., "Main Physical Features and Processes Determining the Performance of Stationary Plasma Thrusters," Journal of Propulsion and Power, Vol. 14, No. 5, 1998, pp. 736–743.

[5]Kaufman, H. R., "Technology of Closed-Drift Thrusters," *AIAA Journal*, Vol. 23, No. 1, 1985, pp. 78–86.

[6]Choueiri, E.Y., "Fundamental Difference Between the Two Hall Thruster Variants," *Physics of Plasmas*, Vol. 8, No. 11, 2001, pp. 5025–5033.

[7]Haas, J. M., Gulczinski, F. S., Gallimore, A> D., Spanjers, G. G., and Spores, R. D., "Performance Characteristics of a 5 kW Laboratory Hall Thruster," AIAA Paper 98-3503, 1998.

[8]Valentian, D., and Maslennikov, N., "The PPS 1350 Probram," Proceedings of the 25th International Electric Propulsion Conference, IEPC 97-134, 1997.

[9]Yamamoto, N., Komurasaki, K. and Arakawa, Y., "Discharge Current Oscillation in Hall Thrusters," *Journal of Propulsion and Power*, Vol. 21, No. 5, 2005, pp. 870-876.

[10]Tahara, H., Goto, D., Yasui, T. and Yoshikawa, T., "Thrust Performance and Plasma Features of Low-Power Hall-Effect Thrusters," *Vacuum*, Vol. 65, No.3-4, 2002, pp.367-374.

[11]Boyd, I. D., "Review of Hall Thruster Plume Modeling," *Journal of Spacecraft and Rockets*, Vol. 38, No. 3, 2001, pp.381-387.

[12]King, L. B., Gallimore, A. D., and Marrese, C. M., "Transport-Property Measurements in the Plume of an SPT-100 Hall Thruster," *Journal of Propulsion and Power*, Vol. 14, No. 3, 1998, pp.327-335.

[13]Tajmar, M., Gonzalez, J., and Hilgers, A., "Modeling of spacecraft-Environment Interactions on SMART-1," *Journal of Spacecraft and Rockets*, Vol. 38, No. 3, 2001, pp.393-399.

[14]Ozaki, T., Inanaga, Y., Nakagawa, T., Kasai, Y., and Matsui, K., "Development status of high power xenon hall thruster of MELCO," 25th International Symposium on Space Technology and Science, ISTS 2006-b-34, 2006.

[15]King, L. B., and Gallimore, A. D., "Ion-Energy Diagnostics in the Plasma Exhaust Plume of a Hall Thruster," *Journal of Propulsion and Power*, Vol. 16, No. 5, 2000, pp.916-922.

[16]King, L. B., and Gallimore, A. D., "Mass Spectral Measurements in the Plume of an SPT-100 Hall Thruster," *Journal of Propulsion and Power*, Vol. 16, No. 6, 2000, pp.1086-1092.

[17]Gulczinski, III, F. S., and Gallimore, A. D., "Near-Field Ion Energy and Species Measurements of a 5-kW Hall Thruster," *Journal of Propulsion and Power*, Vol. 17, No. 2, 2001, pp.418-427.

[18]Gallimore, A. D., "Near- and Far-Field Characterization of Stationary Plasma Thruster Plumes," *Journal of Spacecraft and Rockets*, Vol. 38, No. 3, 2001, pp.441-453.

[19]Kim, S. W., and Gallimore, A. D., "Plume Study of a 1.35-kW SPT-100 Using an ExB Probe," *Journal of Spacecraft and Rockets*, Vol. 39, No. 6, 2002, pp.904-909.

[20]King, L., B., and Gallimore, A. D., "Ion-Energy Diagnostics in an SPT-100 Plume from Thrust Axis to Backflow," *Journal of Propulsion and Power*, Vol. 20, No. 2, 2004, pp.228-242.

[21]Gonzalez, J., and Estublier, D., "Spacecraft/thrusters interaction analysis for SMART-1," International Electric Propulsion Conference, IECP-2005-003, 2005.

[22]Taccogna, F., Longo, S., and Capitelli, M., "Particle-in-Cel with Monte Carlo Simulation of SPT-100 Exhaust Plumes," *Journal of Spacecraft and Rockets*, Vol. 39, No. 3, 2002, pp.409-419.

[23]Oh, D. Y., Hastings, D. E., Marrese, C. M., Haas, J. M., and Gallimore, A. D., "Modeling of Stationary Plasma Thruster Plumes and Implications for Satellite Design," *Journal of Propulsion and Power*, Vol. 15, No. 2, 1999, pp.345-357.

[24]Boyd, I. D., Van Gilder, D. B., and Liu, X., "Monte Carlo Simulation of Neutral Xenon Flows in Electric Propulsion Devices" *Journal of Propulsion and Power*, Vol. 14, No. 6, 1998, pp.1009-1015.

[25]Mikellides, I. G., Jongeward, G. A., Katz, I. and Manzela, D. H., "Plume Modeling of Stationary Plasma Thrusters and Interactions with the Express-A Spacecraft," *Journal of Spacecraft and Rockets*, Vol. 39, No. 6, 2002, pp.894-903.

[26]Yokota, Y., Matsui, M., Sako, D., Nagao, N., Takayanagi, H., Koizumi, H., Komurasaki, K., Arakawa, Y., "Diagnostics of Hall Thruster Plume by Laser Absorption Spectroscopy," 42nd AIAA/ASME/SAE/ASEE Joint Propulsion Conference & Exhibit, AIAA 06-5028, Sacramento, 2006

[27]Matsui, M., Komurasaki, K., and Arakawa, Y., "Laser Absorption Spectroscopy in High Enthalpy Flows," AIAA Paper 05-5325, 2005.

[28]Demtroeder, W., Laser Spectroscopy, 3rd edition, Springer-Verlag, Berlin, 2002.

[29]Deutch, M., "Abel inversion with a simple analytic representation for experimental data," *Applied Physics Letters*, Vol 42, 1983, pp 237-239.

[30]NIST Atomic Spectra Database: http://physics.nist.gov/cgi-bin/AtData/main_asd

[31]Herzberg, G. H., Atomic Spectra and Atomic Structure, DOVER PUBLICATIONS, New York, 1945.